

Polymodal Sensory Transduction in Mouse Corneal Epithelial Cells

Luka Lapajne,¹⁻³ Monika Lakk,¹ Oleg Yarishkin,¹ Lara Gubelj, ¹ Marko Hawlina,^{2,3} and David Križaj^{1,4,5}

¹Department of Ophthalmology & Visual Sciences, University of Utah School of Medicine, Salt Lake City, Utah, United States

²Department of Ophthalmology, University Medical Center, Ljubljana, Slovenia

³Faculty of Medicine, University of Ljubljana, Ljubljana, Slovenia

⁴Department of Bioengineering, University of Utah, Salt Lake City, Utah, United States

⁵Department of Neurobiology & Anatomy, University of Utah, Salt Lake City, Utah, United States

Correspondence: David Križaj, Department of Ophthalmology & Visual Sciences, Moran Eye Center, University of Utah School of Medicine, Salt Lake City, UT 84132, USA; david.krizaj@hsc.utah.edu.

LL and ML contributed equally to the work presented here and should therefore be regarded as equivalent authors.

Received: November 27, 2019

Accepted: January 17, 2020

Published: April 9, 2020

Citation: Lapajne L, Lakk M, Yarishkin O, Gubelj L, Hawlina M, Križaj D. Polymodal sensory transduction in mouse corneal epithelial cells. *Invest Ophthalmol Vis Sci.* 2020;61(4):2. <https://doi.org/10.1167/iovs.61.4.2>

PURPOSE. Contact lenses, osmotic stressors, and chemical burns may trigger severe discomfort and vision loss by damaging the cornea, but the signaling mechanisms used by corneal epithelial cells (CECs) to sense extrinsic stressors are not well understood. We therefore investigated the mechanisms of swelling, temperature, strain, and chemical transduction in mouse CECs.

METHODS. Intracellular calcium imaging in conjunction with electrophysiology, pharmacology, transcript analysis, immunohistochemistry, and bioluminescence assays of adenosine triphosphate (ATP) release were used to track mechanotransduction in dissociated CECs and epithelial sheets isolated from the mouse cornea.

RESULTS. The transient receptor potential vanilloid (TRPV) transcriptome in the mouse corneal epithelium is dominated by *Trpv4*, followed by *Trpv2*, *Trpv3*, and low levels of *Trpv1* mRNAs. TRPV4 protein was localized to basal and intermediate epithelial strata, keratocytes, and the endothelium in contrast to the cognate TRPV1, which was confined to intraepithelial afferents and a sparse subset of CECs. The TRPV4 agonist GSK1016790A induced cation influx and calcium elevations, which were abolished by the selective blocker HC067047. Hypotonic solutions, membrane strain, and moderate heat elevated $[Ca^{2+}]_{CEC}$ with swelling- and temperature-, but not strain-evoked signals, sensitive to HC067047. GSK1016790A and swelling evoked calcium-dependent ATP release, which was suppressed by HC067027 and the hemichannel blocker probenecid.

CONCLUSIONS. These results demonstrate that cation influx via TRPV4 transduces osmotic and thermal but not strain inputs to CECs and promotes hemichannel-dependent ATP release. The TRPV4-hemichannel-ATP signaling axis might modulate corneal pain induced by excessive mechanical, osmotic, and chemical stimulation.

Keywords: TRPV4, corneal epithelium, calcium, ATP, TRPV1

The eye is protected from mechanical injury, desiccation, and microbes by a stratified epithelium that spans the area between a totipotent basal cuboid layer and the corneal surface, and is innervated by A δ -mechanoreceptors and C-type nociceptors from the ophthalmic branch of the trigeminal nerve.¹⁻³ The biomechanical environment (osmotic gradients, extracellular matrix stiffness, intraocular pressure, fluid shear) is important for the function, regeneration, transparency, and pathology of the corneal epithelial (CE) barrier,⁴⁻⁷ which provides resistance to the flow of tear fluid. Osmotically driven transepithelial ion and water gradients impose continual shear (14 dyn/cm²) on corneal epithelial cells (CECs),⁸ whereas abnormal tear tonicity or shear intraocular pressure, contact lens abrasion, and keratoablative interventions can damage epithelial cells, resulting in loss of transparency and overexcitation of corneal afferents.⁶ To alleviate the discomfort, inflammation, and vision loss from mechanically induced corneal injury associated with

opacity, edema, hyperalgesia, and pain, it is necessary to understand how such stressors affect CE mechanoreceptors.

All cells respond to changes in the biomechanical environment with activation of mechanosensing molecules and downstream changes in intracellular signaling and gene expression. A key sensory transduction mechanism, conserved across evolution, are transient receptor potential (TRP) channels, particularly the vanilloid subfamily of nonselective transient receptor potential vanilloid (TRPV)1-4 cation channels ("thermoTRPs") that serve as transducers of cell-intrinsic and extrinsic mechanical, chemical, and temperature stimuli.⁹ The mammalian CE expresses several TRPV isoforms, with TRPV1 implicated in regulation of wound healing,¹⁰ inflammatory signaling,¹¹ and osmotransduction¹²; TRPV3 linked to thermosensing and cell proliferation;¹³ and TRPV4 associated with transduction of moderate temperature, regulatory volume decrease (RVD),¹⁴ and regulation of stemness.¹⁵ However, previous studies tended to be

conducted in immortalized epithelial cell lines¹⁶ in which cells lack native contacts and may have altered their sensory transduction mechanisms. It is therefore important to determine which TRPV channels are expressed and functional in the intact epithelium, how native cells respond to stretch, temperature, and swelling, and whether TRPV activation by extrinsic stressors regulates release of substances that can modulate the firing of trigeminal afferents.

TRPV4 has been identified as a key regulator of mechanically evoked cellular volume regulation, barrier permeability and immune interactions in lung, bladder, esophagus, skin, gut, kidney, choroid plexus, retinal pigment, and ciliary body epithelia.^{17–23} TRPV4-mediated calcium influx has been linked to cytoskeletal reorganization, cell adhesion, formation of focal adhesions, and adenosine triphosphate (ATP)-dependent modulation of afferent excitation in epithelia,^{5,19,24,25} yet mechanisms of TRPV4 gating are both cell-type and context-specific,^{26–29} and the properties of TRPV4 activation in native CECs have not been conclusively established. In this study, we employed imaging, electrophysiological, and molecular approaches to characterize calcium regulation and ATP release in CECs exposed to TRPV4 agonists, strain, volume, and temperature increases. A selective antagonist, HC-067047, was used to inhibit TRPV4 activation, and ATP release from CECs was tracked using the luciferin-luciferase assay. We found that TRPV4 represents a dominant sensory transducer, the activation of which evokes significant transmembrane currents, calcium signals, and hemichannel-dependent ATP release. Moreover, native CECs consist of subpopulations that differ in the response to swelling, temperature, and strain, and in the expression of TRPV1 and TRPV4 channels. By identifying the functional relationships between mechanical stressors, ion channel activation, calcium homeostasis, and purinergic signaling, our findings suggest a new mechanism whereby extrinsic stressors modulate epithelial-afferent interactions in the cornea.

MATERIALS AND METHODS

Ethical Approval and Animals

Animal handling and experiments were conducted in accordance with the National Institutes of Health Guide for the Care and Use of Laboratory Animals, and the ARVO Statement for the Use of Animals in Ophthalmic and Vision Research, with the project also approved by the Institutional Animal Care and Use Committee at the University of Utah. C57BL/6 (C57), TRPV4^{-/-},³⁰ and B6.Cg-Gt(ROSA)26Sortm9(CAGtdTomato) Hze/J (Ai9) in which the LoxP-STOP-LoxP TdTomato construct is knocked in at the Gt(ROSA)26Sor locus (referred to as TRPV1^{tdT})³¹ and bacterial artificial chromosome (BAC)-transgenic Tg(TRPV4-EGFP)MT43Gsat mice (referred to as TRPV4^{eGFP}) mice³² were maintained in a pathogen-free facility with a 12-hour light/dark cycle and unrestrained access to food and water. Data were gathered from 1- to 3-month-old male and female animals with no noted gender differences. A preliminary account of this work was published in an abstract form (Lapajne L, *et al.* IOVS 2019;60:ARVO E-Abstract 916).

Reagents

The TRPV4 agonist GSK1016790A (GSK101) and antagonist HC-067047 (HC-06) were purchased from Sigma (St. Louis,

MO, USA). Suramin and probenecid were obtained from Cayman Chemicals (Ann Arbor, MI, USA). Other salts and reagents were purchased from Sigma, VWR (West Chester, PA, USA), Across Organics (Pittsburgh, PA, USA), or Thermo Fisher (Waltham, MA, USA). GSK101 (1 mM), HC-06 (20 mM), probenecid (50 mM), and suramin (100 mM) stocks were diluted in extracellular saline solution to working concentrations before use. After dissolution in dimethyl sulfoxide (DMSO), the final drug concentrations did not exceed 0.1%.

Tissue Preparation and Cell Culture

Following euthanasia and enucleation, corneas were incubated in Dulbecco's Modification of Eagle's Medium (DMEM)/F12 (1:1 mixture, GIBCO (Grand Island, NY, USA)/Thermo Fisher) containing Dispase II (15 mg/mL, Sigma) and 1% penicillin/streptomycin for 1 hour at 4°C and an additional hour at room temperature. Epithelial sheets were peeled off from the stroma with fine-tipped forceps and used immediately for *in situ* optical imaging experiments. Alternatively, sheets were incubated in DMEM (GIBCO/Thermo Fisher) containing papain (15 U/mL, Worthington (Columbus, OH, USA)) for 30 minutes, rinsed with D-PBS containing 0.5% bovine serum albumin (BSA, Genesee Scientific (San Diego, CA, USA)) and triturated. After dissociation, cells were seeded onto collagen I and fibronectin-coated coverslips (for calcium imaging), or silicon membranes (for stretch experiments). CECs were cultured for 3 to 5 days at 37°C and 7.4 pH in the presence of 5% CO₂ and DMEM/F12 containing 2% fetal bovine serum (FBS), insulin (5 ug/mL), transferrin (10 ug/mL), sodium selenite (5 ug/mL), hydrocortisone (0.5 ug/mL), epidermal growth factor (EGF) (10 ng/mL), fibroblast growth factor (FGF) (10 ng/mL), 1% penicillin/streptomycin, and 1% gentamicin. The cells were identified by immunolabeling with a K12 antibody (Santa Cruz Biotech (Dallas, TX, USA)).

PCR and Semiquantitative Real-Time PCR

Total RNA was isolated from mouse CE sheets using Arcturus PicoPure RNA Isolation Kit (Applied Biosystems (Foster City, CA, USA)) according to the manufacturer instructions. First-strand cDNA synthesis and PCR amplification of cDNA were performed using qScript XLT cDNA Supermix (Quanta Biosciences (Beverly, MA, USA)). The RT-PCR products were run on 2% agarose gels and visualized by ethidium bromide staining, along with 100-base pair DNA ladder (Thermo Scientific). Sybergreen based real-time PCR was performed using Apex qPCR GREEN Master Mix (Genesee Scientific). The comparative C_T method ($\Delta\Delta C_T$) was used to measure relative gene expression in which the fold enrichment was calculated as: $2^{-[\Delta C_T(\text{sample}) - \Delta C_T(\text{calibrator})]}$ after normalization. The results were performed in triplicate of at least four separate experiments and expressed as a relative fold change in gene expression compared with the control. To normalize fluorescence signals, GAPDH and α -tubulin were utilized as endogenous controls. The primer sequences and expected product sizes are given in the [Table](#).

Immunocytochemistry

The immunostaining protocols were as described previously.^{33,34} Briefly, corneas were dissected along the sclero-corneal rim and fixed for 20 minutes in 4%

TABLE. Primer Sequences Used for PCR and Semiquantitative Real-Time PCR Analysis

Name	Forward Primer	Reverse Primer	Product Size (base pair)
<i>Trpv1</i>	AGGGTGGATGAGGTGAAGCTGGACT	GCTGGGTGCTATGCCTATCTCG	199
<i>Trpv2</i>	GTTGGCCTACGTCCTCCTCACCTA	TGACCACCAGTAACCATTCTCC	158
<i>Trpv3</i>	CTCACCTTCGTCTCCTCCTCAAC	CAGCCGGAAGTCTCATCTGCTA	201
<i>Trpv4</i>	TCCTGAGGCCGAGAAGTACA	TCCCCCTCAAACAGATTGGC	166
<i>Gapdh</i>	GGTTGTCTCTCGGACTTCA	TAGGGCCTCTCTCCTCAGT	220
<i>α-tubulin</i>	AAGCAGCAACCATGCGTGA	CCTCCCCAATGGTCTTGTC	145

paraformaldehyde, rinsed 3x with PBS, dehydrated in sucrose solutions (10%-20%-30%), and mounted in optimal cutting temperature compound mounting medium (Electron Microscopy Sciences (Hatfield, PA, USA)). After a quick wash in PBS, the 12- μ m thick cryosections were incubated in a blocking buffer (5% FBS and 0.3% Triton X-100 in 1X PBS) for 20 minutes. Primary antibodies (rabbit anti-TRPV4, 1:1000, LifeSpan Biosciences (Seattle, WA, USA); mouse anti-Pannexin1, 1:100, Santa Cruz Biotech) were diluted (PBS with 2% BSA and 0.2% Triton X-100) and applied overnight at 4°C, followed by 1 hour incubation in fluorophore-conjugated goat anti-rabbit and mouse AlexaFluor 488 and/or 594 secondary antibodies (1:500, Life Technologies) at room temperature. The sections were mounted with DAPI-Fluoromount-G (Southern Biotech (Birmingham, AL, USA)). Images were acquired on Olympus FV1200 confocal microscope (40X objective/0.8 NA water (Tokyo, Japan)) and Fluoview software (Tokyo, Japan) at 1024 \times 1024 pixel resolution.

Patch Clamp and Pressure Clamp Experiments

Whole-cell patch-clamp measurements from primary CECs were conducted with Multiclamp 700B amplifiers, pClamp 10.7 acquisition software, and DigiData 1550 (Molecular Devices (San Jose, CA, USA)) as described in published protocols.^{20,35} The standard extracellular recording solution contained (mM): 140 NaCl, 2.5 KCl, 1.5 MgCl₂, 1.8 CaCl₂, 10 HEPES, 5.5 D-glucose. The pipette solution contained (mM): 120 K-gluconate, 10 KCl, 10 HEPES, 1 MgCl₂, 4 Mg-ATP, 0.6 Na-GTP, 0.5 EGTA, pH was adjusted to 7.3 with potassium hydroxide (KOH). All experiments were performed at room temperature (22°C–23°C). Pipettes were fabricated from borosilicate glass capillaries (World Precision Instruments (WPI), Sarasota, FL, USA; outer diameter 1.5 mm, inner diameter 0.84 mm) and, filled with K-gluconate-based solutions, had resistance of 6 to 9 MOhm. Whole-cell currents were elicited by –100 to 100 mV ramps from the holding potential of –30 mV. RAMP pulses were of 1 second duration and applied at 0.1 Hz. Membrane potential was recorded in the current-clamp mode in which no holding current was applied. The recordings were sampled at 10 kHz and filtered at 5 kHz.

Calcium Imaging

Detached CE sheets and acutely dissociated cells were used for optical imaging as described.^{20,31} Single cells were obtained after enzymatic digestion with papain (15 U/mL) and plated onto coverslips coated with concanavalin A (0.5 mg/mL). Epithelial sheets were carefully peeled off enucleated corneas and placed in the recording chamber (Warner Instruments (Hamden, CT, USA)). Cells/epithelia

were loaded with Fura-2 AM (5–10 μ M, Life Technologies) for 30 to 45 minutes, placed into a recording chamber, and superfused with extracellular saline solution containing (in mM): 133 NaCl, 10 HEPES hemisodium salt, 10 glucose, 2.5 KCl, 2 CaCl₂, 1.5 MgCl₂, 1.25 NaH₂PO₄, 1 pyruvic acid, 1 lactic acid, and 0.5 glutathione at pH 7.4. Extracellular osmolarity was set by addition or removal of mannitol, a procedure that minimally disrupts ionic driving forces and maintains the cells' membrane potentials by maintaining the electrolyte concentrations constant.^{36,37} Solution exchanges were performed via an electronically controlled multibarreled inlet port (Warner Instruments). Fluorescence imaging was conducted with upright and inverted Nikon (Tokyo, Japan) microscope with 40x (1.3 NA oil or 0.80 NA water), and 60x (1.0 NA water) objectives. A total of 340 and 380 nm excitation was delivered via a Xe lamp (Lambda DG-4; Sutter Instruments (Novato, CA, USA)). Emission was collected at 510 nm with 14-bit CoolSNAPHQ2 or Delta Evolve cameras (Photometrics (Tucson, AZ, USA)). Backgrounds were subtracted and F₃₄₀/F₃₈₀ ratios computed with NIS-Elements software (Nikon); $\Delta R/R$ (peak F₃₄₀/F₃₈₀ – baseline/baseline) was used to quantify the amplitude of Ca²⁺ signals,^{38,39} in which R is the ratio of emission intensity at 510 nm evoked by 340 nm excitation versus emission intensity at 510 nm evoked by 380 nm excitation. The results represent averages of responses from cells from at least three animals and three independent experiments.

Cyclic Tensile Force Application

CECs were plated onto silicon membranes coated with collagen type I and cultured for 3–5 days. The membranes were placed into computer-controlled, vacuum-operated Flexcell FX-4000 System (Flexcell International Corporation (Burlington, NC, USA)) and loaded with Fura-2-AM (5–10 μ M, Life Technologies) for 30 to 45 minutes, with HC-06 (1 μ M) or the vehicle (<0.001% DMSO) added 1 hour prior to stretch. Cyclic equiaxial stretch (10%, 1.0 Hz) was applied for 10 minutes at 37°C,⁴⁰ whereas control cells were plated on membranes but not subjected to stretch. The cells were imaged with Nikon E600FN upright microscopes and a 40x (0.8 NA water) objective, and data acquisition was controlled by Nikon Elements (Tokyo, Japan).

ATP Detection

The extracellular ATP released from CECs was quantified using the bioluminescence detection assay from Cayman Chemicals (ATP Detection Assay Kit; No. 700410). ATP concentrations for each well were calibrated using a standard concentration curve established with NaATP (Cayman Chemicals). Dissociated cells were treated with GSK101, hypotonic stimulation (HTS), probenecid, and/or suramin

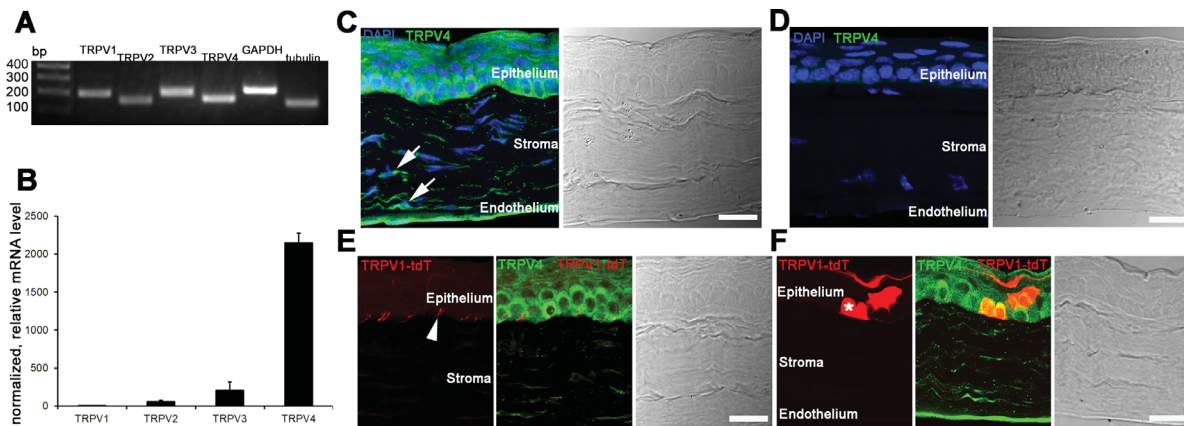


FIGURE 1. TRPV4 channel expression and localization in mouse corneal epithelium. (A) PCR analysis of *Trpv* transcripts in the mouse corneal epithelium, with *Gapdh* and α -tubulin as loading controls. (B) Tabulated semiquantitative RT-PCR data, shown as \sim fold changes of *Trpv* mRNA relative to *Trpv1* ($n = 4$). (C–F) Transmitted and fluorescent CE images; vertical sections labeled for TRPV4. (C) Epithelial TRPV4-ir shows a basal-to-squamous gradient, with additional immunosignals in the endothelium and stromal keratinocytes (arrows); (D) these signals are absent in TRPV4^{-/-} corneas. (E, F) TRPV1Cre/Ai9 corneas. (E) Central CE. tdT, a TRPV1 lineage reporter, labels thin subbasal TRPV4-immunonegative processes (arrowhead). (F) Limbal CE. tdT localizes to a small subset of TRPV4-ir epithelial somata (asterisk) but is absent from keratinocytes and endothelial cells. Scale bars: 20 μ m. bp, base pair.

in the presence of the NPTDase inhibitor ARL 67156 (100 μ M, Tocris (Bristol, UK)) for 10 minutes. At the end of the treatments the samples were centrifuged at 400g, 1000g for 5 minutes at 4°C to pellet floating cells and supernatants. The supernatants were transferred to a white plate for single photon counting of luciferin-luciferase luminescence (Microplate Multimode Reader, Turner Biosystems (Pittsburgh, PA, USA)).

Data Analyses

Statistical analysis was performed using Origin Pro 8.5 (Northampton, MA, USA). Data were acquired from at least three independent experiments. Results are given as mean \pm SEM. Unpaired sample *t*-test was used to compare two means, and 1- or 2-way ANOVA with Tukey's test to analyze three or more means. $P > 0.05 =$ nonsignificant (N.S.), $P \leq 0.05 = *$, $P \leq 0.01 = **$, $P \leq 0.001 = ***$, $P \leq 0.0001 = ****$.

RESULTS

TRPV4, the Dominant thermoTRP Isoform in CECs, is Distributed in a Nonuniform Manner

Vanilloid thermoTRP channels (TRPV1–4) sense a range of environmental cues relevant for the mouse cornea.⁴¹ To gain insight into the mouse CE sensome, we first analyzed the relative expression of *Trpv* transcripts amplified from CE sheets. Semiquantitative RT-PCR showed that CEC expression is dominated by *Trpv4*, followed by *Trpv3* and *Trpv2*, whereas *Trpv1* expression was low (Figs. 1A, 1B, and Supplementary Fig. S1).

Antibody labeling was used to map TRPV4 distribution across the corneal epithelium, with absence of staining in TRPV4^{-/-} corneas used to validate the signals. TRPV4 immunoreactivity within the epithelium was characterized by prominent labeling of the basal layer (composed of unipotent and recycling stem cells) and intermediate strata, and weak labeling of superficial layers (Figs. 1C, 1E–F). A similar expression pattern was observed in corneas from

transgenic TRPV4^{eGFP} animals that express a fluorescent reporter under the control of the TRPV4 promoter^{32,34} (Supplementary Fig. S2). As in other epithelia,⁴² the subcellular distribution of TRPV4-ir included plasma membrane and cytosolic signals. TRPV4^{-/-} corneas stained for TRPV4 showed little labeling and few discernible changes in overall architecture (Fig. 1D), indicating that TRPV4 function is not required for epithelial development. Consistent with previous observations,¹² TRPV4-ir was also seen in the endothelium and stromal keratinocytes (Fig. 1C).

TRPV1 was reported to be the dominant thermoTRP variant in cultured human CECs.¹² Given the unreliability of TRPV1 antibodies,³¹ we evaluated TRPV1 expression in TRPV1Cre: Ai9 corneas in which TRPV1 expression manifests as tdTomato fluorescence.^{34,43} Figure 1E shows that the majority of CECs lacks tdT expression. Indicating low *Trpv1* mRNA expression in the mouse CE (Fig. 1B), tdT reporter signals were confined to a small subset of basal and intermediate CECs that seemed to be more prevalent in the limbal CE (Fig. 1F). TRPV1-expressing cells were always TRPV4-ir. In addition, we observed TRPV1 signals in processes that emanate from the stroma into the epithelium (arrowheads, Fig. 1E), presumably corresponding to polymodal nociceptive afferents.⁴⁴ These data demonstrate strong TRPV4 expression in mouse CE, keratinocyte, and endothelial cells, whereas TRPV1 might be localized to subsets of CECs and trigeminal nerve endings.

CECs Constitutively Express a Functional TRPV4 Channel

To evaluate TRPV4 functionality in the absence of nonautonomous factors, dissociated CECs were loaded with the Ca²⁺ indicator Fura-2-AM (5–10 μ M) and exposed to the selective synthetic agonist GSK1016790A (GSK101). The protocol evoked robust calcium mobilization that was plotted as background-subtracted ratios ($\Delta R/R$) and percentage of agonist responding cells. In aggregate, GSK101 (25 nM) elevated [Ca²⁺]_i with $\Delta R/R = 1.04 \pm 0.25$ ($N = 4$; $n = 39/89$ cells) (Figs. 2A, 2B), an effect that was abolished by

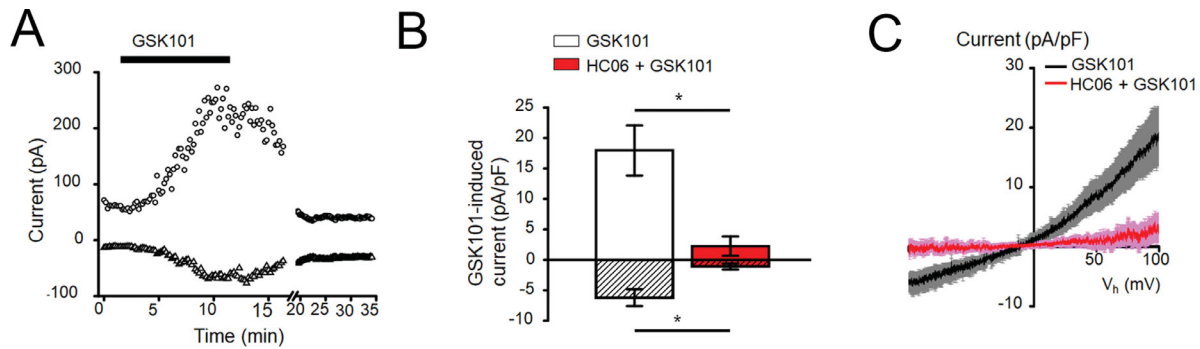


FIGURE 2. Functional expression of TRPV4-mediated calcium influx. Acutely dissociated cells loaded with Fura-2 AM. (A) Averaged GSK101-elicited $[Ca^{2+}]_i$ response from 10 cells (black trace); the agonist response is blocked by HC-06 (red trace, $n = 10$). (B) Individual CEC response traces for the experiment shown in A. \pm SEM.

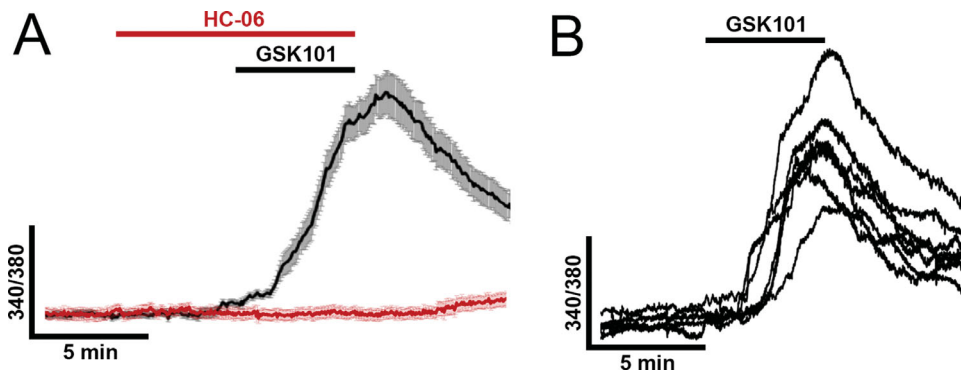


FIGURE 3. Functional expression of the TRPV4-mediated current. Acutely dissociated cells. (A) Representative time-course of the whole-cell current recorded at the holding potential -100 mV (triangles) and $+100$ mV (circles) show slow onset, sustained responses to the agonist GSK101. (B) Summary of GSK101 responses in CECs. The antagonist HC-06 inhibits inward and outward current components evoked by GSK101 at -100 and $+100$ mV, respectively. (C) GSK101-induced current (black trace) shows a quasilinear I-V relationship, reversal near 0 mV, and inhibition by HC-06 (red trace). \pm SEM. $n = 9$; $*P < 0.05$.

pretreatment with the selective antagonist HC-067047 (HC-06), $1\mu\text{M}$ (Fig. 2A).

To gain insight into the kinetics of channel activation, we recorded membrane current in whole-cell clamped cells. GSK101 induced nonselective cation currents that reversed at -13.9 ± 14.8 mV ($n = 9$) (Figs. 3A, 3B). The inward and outward components of agonist-evoked currents recorded at negative (-100 mV) and positive ($+100$ mV) holding potentials (red traces and bars in Figs. 3B, 3C) were reversibly inhibited by HC-06 ($n = 9$), with the average inward current attenuated from -6.22 ± 1.38 pA/pF to -1.09 ± 0.49 pA/pF ($P < 0.05$), and the outward component reduced from 17.96 ± 4.12 pA/pF to 2.24 ± 1.6 pA/pF ($P < 0.05$), 82.5% and 87.5% decreases, respectively (Fig. 3B). Hence TRPV4 is functionally expressed in the mouse CEC plasma membrane.

The Intact Epithelium Shows Ca^{2+} -Dependent Propagation of Calcium Signals

We next assessed the properties of CE TRPV4 activation in situ by conducting imaging experiments in whole-mount sheets that had been peeled off the corneal stroma. Similar to cells in isolation, GSK101 evoked increases in free $[Ca^{2+}]_i$ in intact CECs (Figs. 4A, 4B, 4C panel iv). On

average, GSK101 elevated $[Ca^{2+}]_i$ $\Delta R/R$ by 0.98 ± 0.03 ($N = 3$; $n = 103$; $P < 0.0001$), whereas HC-06 inhibited it to 0.15 ± 0.01 ($N = 3$; $n = 87$; $P < 0.0001$) (Figs. 4A–C). GSK101-induced $[Ca^{2+}]_i$ signals were defined by slow onset, delayed peak $[Ca^{2+}]_i$ amplitude (~ 5 minutes after onset), weak inactivation, and gradual increase in the overall fluorescence signal (Fig. 4C panel vii) that may reflect differential expression of TRPV4 across cells (Fig. 1). HC-06 had no effect on baseline $[Ca^{2+}]_i$, indicating that TRPV4 is not activated tonically, but blocked agonist-induced calcium signals (Figs. 4A, 4B) ($N = 3$; $n = 78$; $P < 0.0001$).

CE TRPV4 Channels are Activated by Hypotonic Stimuli but do not Mediate RVD

TRPV4 was originally identified as a systemic and cellular osmosensor owing to its activation by cell swelling,⁴⁵ with TRPV4-dependent Ca^{2+} influx implicated in driving RVD in human CECs.¹⁴ We probed its osmoregulatory functions in mouse cells using anisotonic gradients generated by addition/removal of mannitol at constant ionic strength (see Materials and methods). HTS induced by lowering saline tonicity from 300 ± 5 mOsm to 190 mOsm

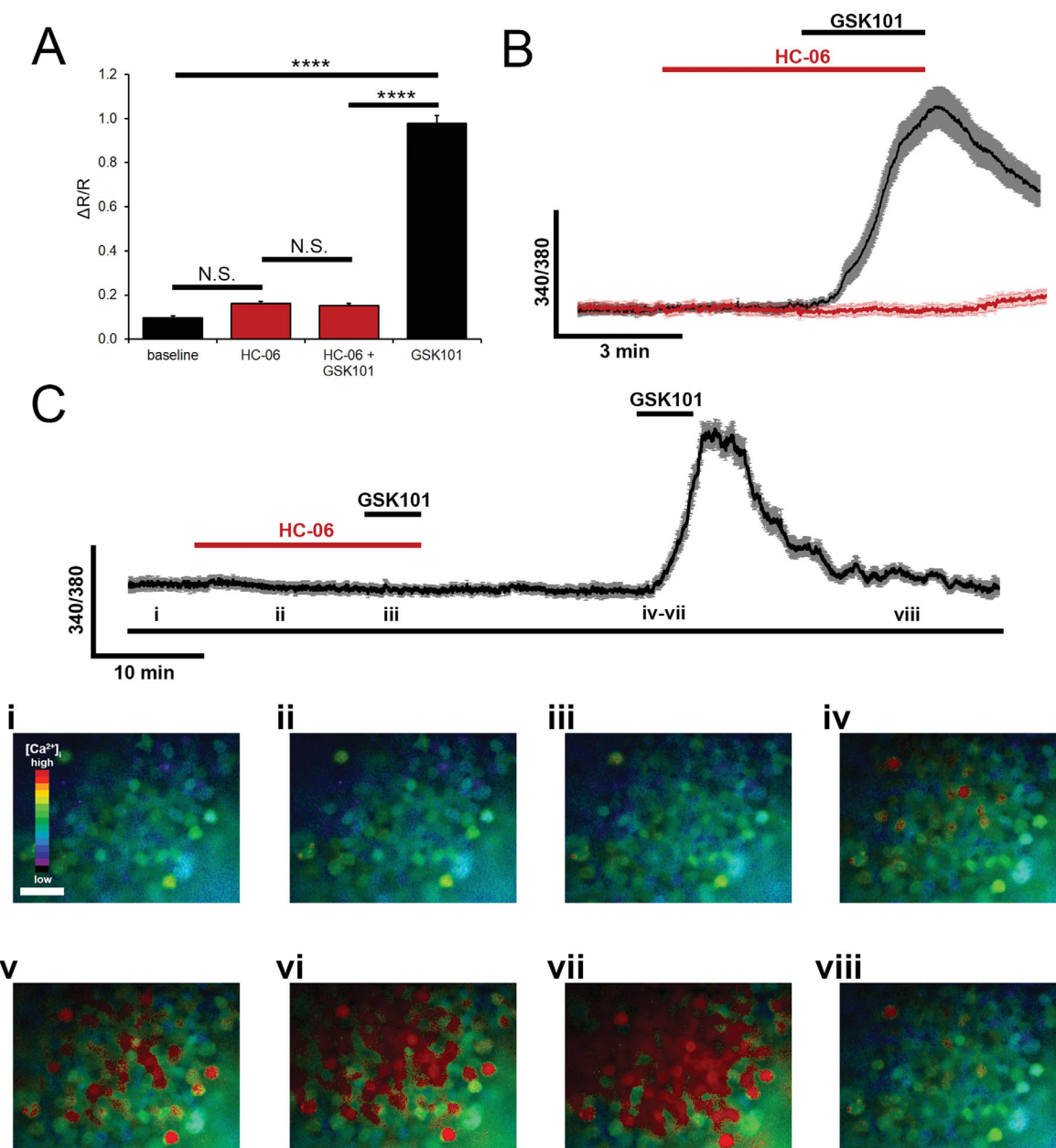


FIGURE 4. Intact epithelial sheet. TRPV4 mediates $[Ca^{2+}]_i$ elevations in the majority of CECs. Calcium imaging. (A) GSK101 (25 nM)-evoked $[Ca^{2+}]_i$ increases are attenuated by HC-06 ($n = 87$, $N = 3$). (B) Summary of TRPV4-mediated signals ($n = 10$). (C) Representative experiment. GSK101 has no effect in the presence of HC-06 but evokes calcium signals on its own. The time points under the trace correspond to ratiometric images shown in panels Ci-viii. **** $P < 0.0001$; N.S., nonsignificant. Scale bar: 30 μm .

(~35% osmolarity decrease) evoked sustained and reversible $[Ca^{2+}]_{CEC}$ signals, with $\Delta R/R$ increase of 0.32 ± 0.01 ($N = 3$; $n = 86$; $P < 0.0001$) (Fig. 5A). To unmask potential RVD mechanisms, CECs were exposed to 140 mOsm saline solution (54% osmolarity decrease), which evokes RVD in fibroblasts⁴⁶ and glia.³⁶ Under these conditions, $\Delta R/R$ increased by 0.44 ± 0.01 ($N = 3$; $n = 105$; $P < 0.0001$) yet little RVD was observed within the 15 minute time frame. To determine the TRPV4-dependence of swelling-induced Ca^{2+} signals, cells were stimulated with HTS in the presence of the channel blocker HC-06 (Figs. 5C, 5D panel i, 5D panel iii). Under these conditions, the amplitude of HTS-evoked calcium responses was significantly ($P < 0.0001$) reduced

($\Delta R/R = 0.25 \pm 0.08$; $N = 3$; $n = 100$), however, the cells also exhibited a transient residual $[Ca^{2+}]_i$ signal (Figs. 5C, 5D panel i) that indicates activation of auxiliary volume regulation mechanisms.

Cultured human CECs respond to shrinking with activation of TRPV1 channels,^{12,14} and TRPV1 knockout mice show impaired responses to hypertonic challenges.⁴⁷ To determine whether this mechanism is functional in the mouse, CECs were exposed to 450 mOsm saline solution (~50% increase in tonicity). The hypertonic stimulus had no effect on $[Ca^{2+}]_{CEC}$ ($\Delta R/R = 0.21 \pm 0.01$; $N = 3$; $n = 121$) (Fig. 5B), indicating that mouse CECs do not employ TRP channels to transduce cell shrinking and/or express the

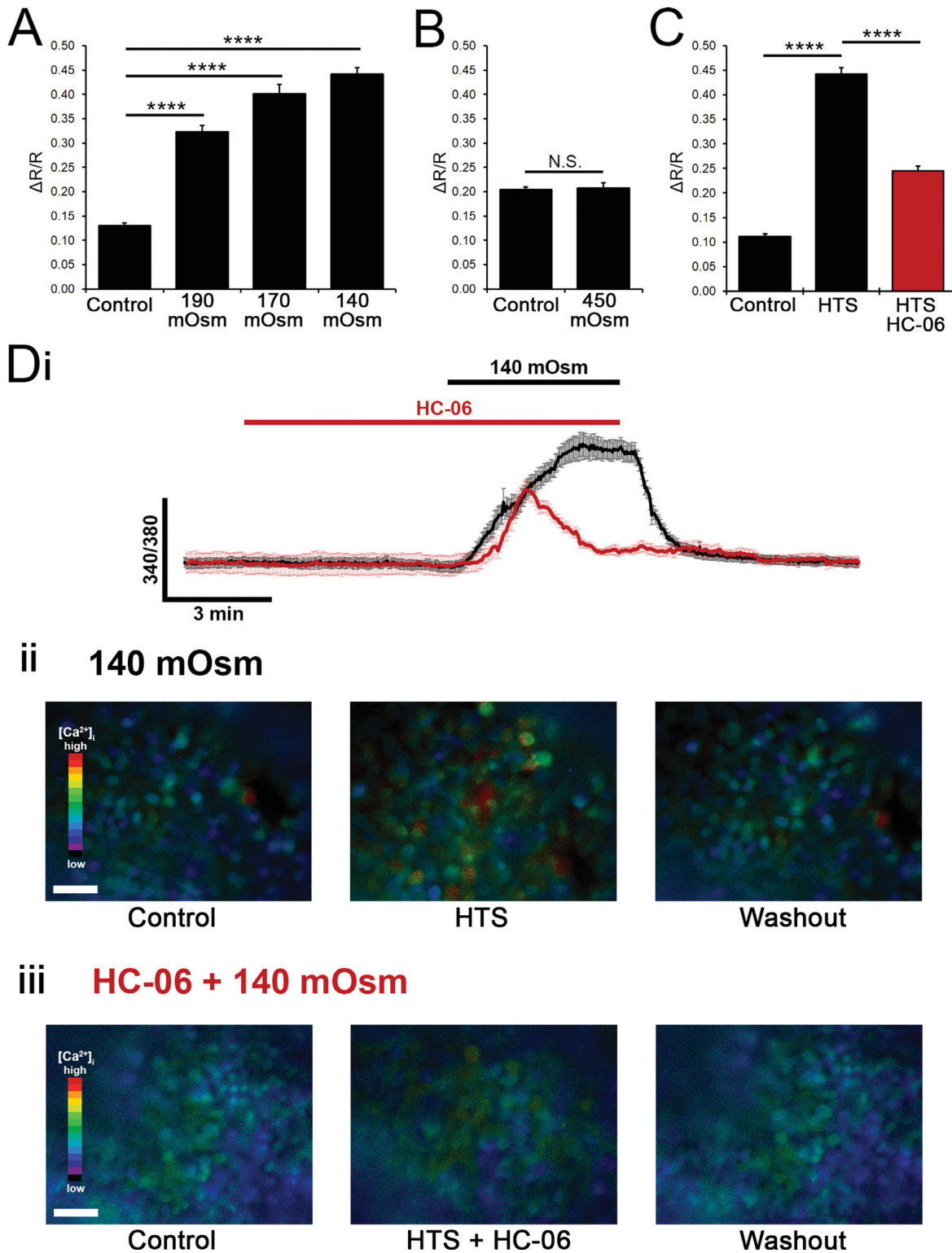


FIGURE 5. Intact epithelial sheet. TRPV4 functions as CEC osmosensor. Calcium imaging. (A) HTS evoke dose-dependent increases in [Ca²⁺]_i, whereas (B) hypertonicity (450 mOsm saline) has no effect. (C) Data summary from four HTS-treated preparations; HC-06 attenuated [Ca²⁺]_i increases induced by 140 mOsm saline. (D) (i) Representative trace from HTS (140 mOsm)-exposed cells in the presence (red trace) and absence (black trace) of HC-06 (*n* = 12). The antagonist treatment unmasked a residual, transient, HC-06-resistant [Ca²⁺]_i response. (ii) Ratiometric images from control (Di; black trace), and (iii) HC-treated (Di; red trace) cells. ± SEM. *****P* < 0.0001; N.S., nonsignificant. Scale bars: 30 μm.

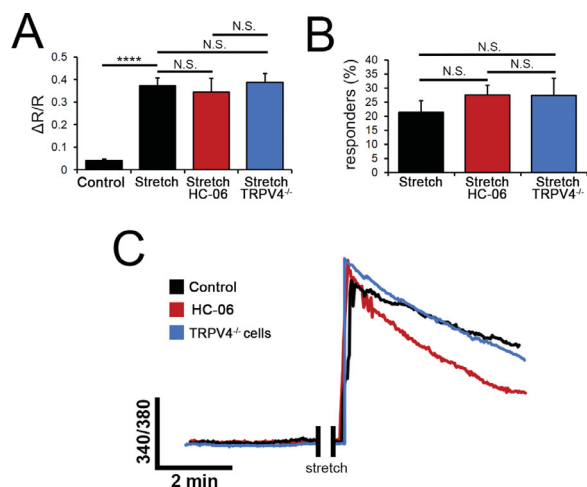


FIGURE 6. Strain evokes $[Ca^{2+}]_i$ responses that are independent of TRPV4. Calcium imaging. Dissociated CECs were cultured on silicon membranes and exposed to cyclic stretch (1.0 Hz, 10%). Acquisition was paused during the stretch owing to loss of focus. (A) Stretch-evoked $[Ca^{2+}]_i$ responses in wild type (WT) (black trace), HC-06-treated (red trace), and TRPV4^{-/-} (blue trace) cells show comparable amplitudes and kinetics. (B, C) Summary ($N = 21$; $n = 10$ –25 cells per experiment). The amplitudes and fractions of stretch-evoked $[Ca^{2+}]_i$ increases are comparable between wild type controls, HC-06-treated and TRPV4^{-/-} cells. **** $P < 0.0001$; N.S., nonsignificant.

truncated ΔN -TRPV1 homolog that serves as the hypertonicity sensor.⁴⁸

TRPV4 Mediates Heat- but not Strain-Induced Changes in Intracellular Calcium

CECs are subjected to mechanical strain from intraocular pressure and eyelid movements⁶ but it is not known whether substrate deformations affect their calcium homeostasis. To

test this, cells were seeded onto silicon membranes, loaded with the indicator dye, and exposed to periodic substrate displacement (1.0 Hz, 10% elongation, 10 minutes). Radial stretch evoked reversible $[Ca^{2+}]_i$ elevations ($\Delta R/R = 0.37 \pm 0.04$; $N = 7$; $n = 157$) in a subset (~22%) of cells. Surprisingly, HC-06 had no effect on the percentage of responding cells (~26%), peak amplitude ($\Delta R/R = 0.35 \pm 0.06$), time-dependence, or the waveform of stretch-evoked $[Ca^{2+}]_i$ responses ($N = 6$; $n = 89$) (Figs. 6A–C). CECs isolated from *Trpv4*^{-/-} animals showed comparable ($P = 0.734$) $[Ca^{2+}]_i$ increases ($\Delta R/R = 0.38 \pm 0.04$; $N = 8$; $n = 138$) in a similar fraction (~27%) of cells (Figs. 6A–C). Hence CECs respond to physiological strains with Ca^{2+} signals that are not mediated by TRPV4 channels.

Temperature is an important stimulus parameter for the cornea, with local gradients reflecting heat emitted from choroidal blood flow and convectional flow of the aqueous humor.⁴⁹ We therefore investigated the effect of physiological temperature on mouse CEC calcium homeostasis in cells that were subjected to transient temperature elevations from 24°C to 37°C (see Materials and methods). Approximately 20% of cells responded to warm saline solution with transient $[Ca^{2+}]_i$ increases, whereas slow progressive $[Ca^{2+}]_i$ elevations were observed in approximately 80% of cells (Figs. 7A, 7B). Evoked $\Delta R/R$ ratios (0.18 ± 0.01 ; $N = 5$; $n = 96$; $P < 0.0001$) were moderately yet significantly ($P < 0.001$) attenuated by HC-06 ($\Delta R/R = 0.14 \pm 0.01$; $N = 4$; $n = 75$) (Figs. 7C, 7D). Hence the CEC $[Ca^{2+}]_i$ response to moderate heat includes a TRPV4 component.

TRPV4 Activation Drives ATP Release

The data presented so far show that cell swelling induces cation influx through TRPV4 channels, and that TRPV4 activation results in spread of calcium signals across the epithelium. If increases in $[Ca^{2+}]_i$ trigger the release of extracellular modulators that are important for corneal physiology, such as ATP,⁵⁰ these should be evident in supernatant tested with the luciferin-luciferase assay,^{24,51} normalized relative to the

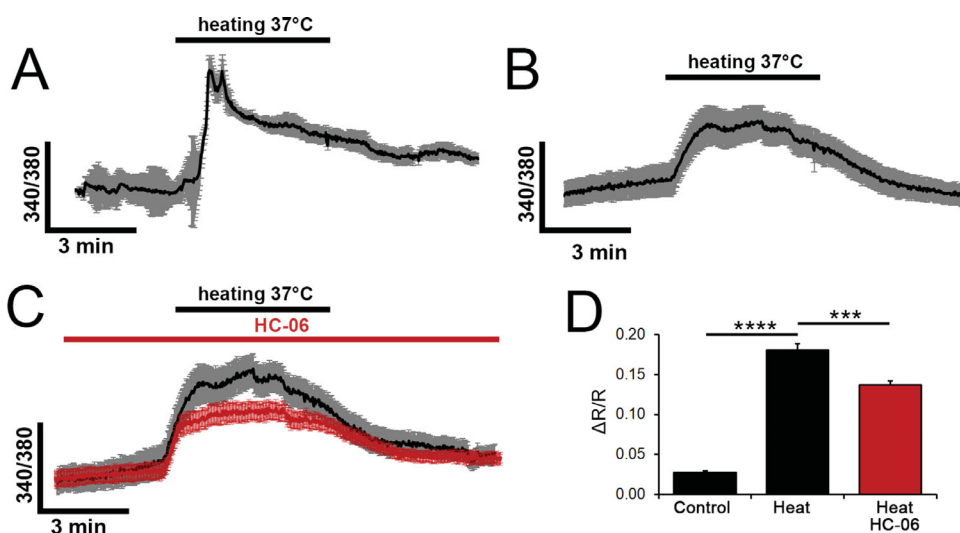


FIGURE 7. TRPV4 functions as a core body temperature sensor. Acutely dissociated CECs. (A) Temperature steps from 22°C to 37°C elevate $[Ca^{2+}]_{CEC}$. A subset (~20%) of responding cells displayed a “fast” $[Ca^{2+}]_i$ response that followed by a sustained plateau. (B) The majority of cells (~80%) showed a sustained “slow” response without the peak. (C, D) HC-06 suppressed the rapid component and reduced the amplitude of heat-evoked $[Ca^{2+}]_i$ increases (red trace and bar) relative to control cells (black trace and bar). \pm SEM, **** $P < 0.0001$.

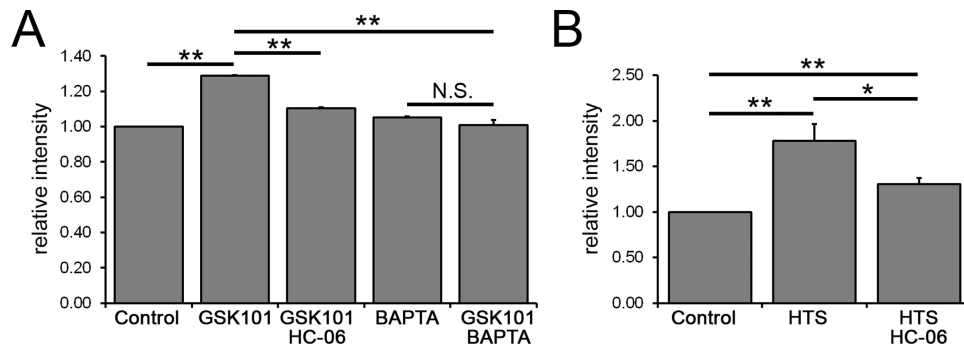


FIGURE 8. GSK101 and HTS drive TRPV4- and calcium-dependent purinergic signaling. Luciferin-luciferase assay in wells seeded with CECs (A) GSK101-induced increases in ATP release were antagonized by HC-06 (1 μ M) and BAPTA-AM (100 μ M) ($N = 3$). (B) Similarly, HC-06 significantly attenuated ATP release in response to HTS ($N = 3$). * $P < 0.05$, ** $P < 0.01$, N.S., nonsignificant.

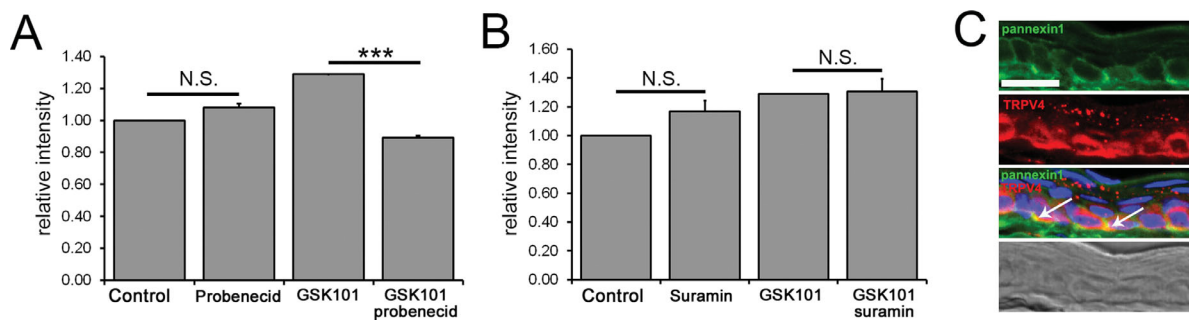


FIGURE 9. ATP release requires Pannexin hemichannels. Luciferin-luciferase bioluminescence assay. Supernatants from GSK101-treated wells. (A) GSK101-evoked ATP release is antagonized by the hemichannel blocker probenecid (50 μ M) ($N = 3$). (B) The P2 receptor blocker suramin does not affect GSK101-evoked ATP release ($N = 3$). (C) TRPV4-ir (Alexa 594 nm) colocalizes with Pnx1-ir signals (Alexa 488 nm) (arrowheads). *** $P < 0.001$, N.S., nonsignificant Scale bar 20 μ m.

calibration standards (see Materials and methods). As illustrated in Figure 8, 10 minute exposure to GSK101 increased [ATP] within the supernatant to 1.29 ± 0.00 ($P < 0.01$) (Fig. 8A), an effect that was abolished by HC-06 to 1.10 ± 0.01 ($P < 0.01$). TRPV4-induced ATP release was also abrogated by the fast membrane-permeable Ca^{2+} chelator BAPTA-AM (100 μ M). Consistent with its role in TRPV4 activation, HTS-evoked HC-06-sensitive ATP release. In the presence of the antagonist, the supernatant signal was reduced from 1.78 ± 0.18 to 1.30 ± 0.07 ($N = 3$; $P < 0.05$; Fig. 8B).

TRPV4-Induced ATP Release Requires Pannexins

Previous studies showed that TRPV4-mediated ATP release in nonexcitable cells involves exocytotic, hemichannel, and/or P2 purinergic mechanisms.^{52–54} Given that Pannexin1 (Pnx1) hemichannels are activated by intracellular calcium, permeable to ATP and may functionally couple to TRPV4,⁵² we evaluated ATP release in the presence of probenecid, at the concentration (50 μ M) that blocks hemichannels without affecting gap junctional coupling or TRPV2 activation.^{55–58} As shown in Figures 9A, 9B, GSK101-evoked increases in extracellular [ATP] were reduced in the presence of probenecid from 1.29 ± 0.00 to 0.89 ± 0.01 ($P < 0.001$). We tested the possibility that TRPV4-mediated ATP release involves purinergic autocrine feedback⁵⁹ but the bioluminescence signal intensity in the presence of the P2 receptor blocker suramin (100 μ M) was 1.31 ± 0.09 , not signif-

icantly different from the GSK101-alone cohort. Consistent with Pannexin involvement, CEC TRPV4-ir colocalized with Pnx1, which showed similar preferential localization to the basal stratum (Fig. 9C). Taken together, these results suggest that hemichannels contribute to TRPV4-dependent purinergic signaling in the corneal epithelium.

DISCUSSION

This study provides insight into the molecular mechanisms that mediate CE sensing of mechanical, temperature, osmotic, and chemical stimuli. We found that (1) *Trpv4* dominates vanilloid thermoTRP transcript expression in primary mouse CECs; (2) translayer TRPV4 expression is nonuniform, with a pronounced gradient from basal to superficial epithelial layers; (3) TRPV4 activation shows a uniquely polymodal activation pattern that is characterized by the sensitivity to osmotic swelling and core temperatures but not cell shrinking and strain; (4) CEC TRPV4 activation drives hemichannel-dependent ATP release; and (5) only a subset of basal/intermediate cells and afferent nerve endings express TRPV1. Our results suggest that TRPV channels and calcium homeostasis contribute to CE integration of mechanical, temperature, and chemical inputs. Previous studies have shown that cultured CECs express TRPV1–4 channels and respond to hyper/hypotonic stimuli,^{11,13,14} but to our knowledge this is the first study to demonstrate

calcium signaling in CE sheets in which cells maintain their connections and signaling mechanisms.

RNA profiling of the mouse corneal epithelium suggests that it responds to sensory inputs via multiple transducers, as indicated by vanilloid transcripts that were dominated by *Trpv4*, followed by modest levels of *Trpv2/Trpv3*, and a low amount of *Trpv1* mRNA. Consistent with prominent transcript expression, immunohistochemistry showed robust TRPV4 expression in central and limbal regions and a well-defined basal-to-squamous gradient of TRPV4-ir and TRPV4^{eGFP}, a pattern that resembles the basal-apical TRPV4 expression patterns reported in urothelial, skin, and mammary epithelia,^{17,18,60} but differs from the rabbit cornea in which TRPV4 was localized to apical cells.⁶¹ Basal expression implicates TRPV4 in differentiation/stemness and/or barrier permeability functions,^{15,21,33} whereas plasma membrane TRPV4-ir reflects the well-known roles of the channel in ion transport, Ca²⁺ homeostasis, and volume regulation.^{45,62,63} Although the function of cytosolic TRPV4-ir puncta is less clear, total internal reflection microscopy studies have linked such puncta to stimulus- and development-dependent trafficking of endosomes, membrane translocation, insertion, and/or internalization.^{64–68} Given that TRPV4 is expressed in the CE,^{12,14} afferents,¹⁵ fibroblasts,⁶⁹ stromal keratocytes,⁷⁰ and the endothelium (Fig. 1) it probably functions as a pan-corneal regulator of sensory inputs.

Similar to TRPV4, TRPV1 expression was largely confined to basal and intermediary epithelium, a pattern that differs from human corneas in which TRPV1 was reported to be localized to superficial strata. Although capsaicin receptor transcripts represent the most abundant vanilloid mRNAs in the human tissue, we find its expression in the mouse CE to be modest, with reporter expression in TRPV1^{tdT} corneas confined to a subset of CECs that may endow the CE with sensitivity to anandamide, protons, noxious heat, and capsaicin.^{31,71,72} TdT always colocalized with TRPV4 but it remains to be seen whether the vanilloid subunits heteromerize, as recently reported for endothelial cells⁷³ but not retinal ganglion cells.³⁴ Consistent with the latter possibility, barrier permeability in CE monolayers is regulated by GSK101 but not the TRPV1 agonist capsaicin.⁶¹ Our finding that mouse CECs do not respond to hypertonic stimuli may reflect the rareness of TRPV1-expressing cells, low TRPV1 expression in adult tissue, and/or presence of full-length protein variants that are not activated by cell shrinking.⁴⁸ We detected TRPV1 reporter signals in a subset of nerve ending-like processes, an observation that accords with histological and functional studies showing heat-, hypertonicity- and mechano-dependent firing in a capsaicin- and hypertonicity-responding population of polymodal nociceptor afferents.^{2,44} It is not clear whether discrepancies in TRPV expression across human, rabbit, and mouse CE models reflect species differences, differential signaling in normal versus immortalized cells, and/or altered pain sensing across species.

Many features of cellular signaling can be inferred from the kinetics and activation properties of transmembrane currents and calcium signals. The whole-cell currents and [Ca²⁺]_i elevations that are evoked in dissociated, cultured, and whole-mount CEC preparations by GSK101 and hypotonic swelling indicate robust functional expression of the TRPV4 protein. Consistent with differences in TRPV4-ir across strata (Fig. 1), we found the peak amplitude and kinetics of TRPV4-mediated responses to vary across cells.

It is possible that faster and larger responses correspond to basal cells, which express channels at high densities and may utilize them to propel regeneration.¹⁵ Because TRPV4-mediated currents and [Ca²⁺]_i elevations took several minutes to peak, we hypothesize that the channel is gated by intermediary mechanisms, such as phospholipase A2, phosphatidylinositol phosphate, and/or eicosanoid metabolites that require minutes lag time for activation.^{24,40,74–76,77}

Dry eye treatments rely on hypotonic artificial tears to counter evaporative water loss and epithelial cell damage,^{8,78} and are therefore likely to trigger mechanisms that sense CEC swelling. We found that sustained TRPV4-mediated increases in [Ca²⁺]_{CEC} evoked by hypotonic gradients lead to massive ATP release, indicating functions in epithelial osmoregulation, volume sensing, and purinergic signaling.^{45,52,63} It is thus possible that increased hydration associated with CE swelling (edema) caused by accidental or surgical injury might elevate [Ca²⁺]_{CEC} in a TRPV4-dependent manner. We recently found that such activations can be augmented by water fluxes through aquaporin channels, which drive time-dependent facilitation of TRPV4 activation via the N-terminal domain of the protein.^{29,36} Overactivation of this mechanism in CECs, which utilize AQP5 to regulate corneal thickness and water transport across the epithelial barrier,⁷⁹ could contribute to edema by triggering the positive feedback loop between cell swelling, calcium overloads, purinergic excitation, and fluid dysregulation.^{80,81} The transient, HC-06-resistant component of hypotonicity-evoked [Ca²⁺]_i increases remains to be identified but could involve release of calcium from internal stores or activation of recently identified OSCA/TMEM63 channels.^{82,83}

Interestingly, dissociated CE cells and cells within the intact tissue varied in functional expression of TRPV4 and responsiveness to swelling, thermal, and/or strain stimuli. The stressors elevated [Ca²⁺]_i, yet only the effects of swelling and temperature but not strain were sensitive to HC-06, suggesting that ambient inputs are sensed by parallel transducers that are differentially distributed across CECs. The residual response to moderate heat, observed in the presence of the TRPV4 blocker, may involve TRPV3 channels, which are expressed in mouse CECs (Fig. 1).¹³ Because these isoforms are optimally activated at core body temperatures, TRPV3 and TRPV4 might mediate tonic Ca²⁺ influx in vivo. Physiological levels of cyclic strain (10%) evoked similar [Ca²⁺]_i amplitudes and responder fractions (~20%–25%) in wild type, *Trpv4*^{-/-} and HC-06-inhibited cells, suggesting that (1) CEC strain sensing is independent of TRPV4; (2) confined to a small subset of CECs; and (3) differs from cell types that utilize TRPV4 channels to sense substrate deformation (endothelial, chondrocyte, trabecular meshwork, and pulmonary epithelial cells).^{40,84–86} The simplest explanation, that TRPV4 activation reflects the unique lipid and signaling aspects of the CEC microenvironment, is supported by the remarkable spectrum of TRPV4 activation mechanisms across cells and tissues.^{26,28,29} Phospholipase A2 activation is required for TRPV4 gating in glia, nonpigmented cells of the ciliary body, and recombinant HEK293 cells but not neurons and heterologously expressing oocytes,^{20,26–28} whereas membrane stretching in response to positive pressure activates TRPV4 in glia and oocytes but not chondrocytes.^{26,85,87} The structural determinants that regulate the differential responsiveness remain to be fully elucidated, with existing evidence indicating multisite regulation: residues from S2-S3 and S4-S5 linkers encode its sensitivity to eicosanoids,⁸⁸ TM3-4 regions control responses

to agonists and heat,⁸⁹ whereas CYP450 enzymes regulate responsiveness to polyunsaturated lipids.⁷⁷ Our recent study suggests that differential responsiveness to osmotic stress involves binding of the N-terminus to cytoskeletal/membrane structures that mimic PLA2-bound protein conformations of the channel.²⁹ Further studies are required to delineate the molecular determinants that control how the CEC TRPV4 channels respond to extrinsic and intrinsic stressors, and whether lack of activation by strain involves masking of the N-terminal region by PACSIN SH3 domains.⁹⁰

The present study identifies the TRPV4-hemichannel-ATP signaling axis as a potential modulator of paracrine, mechanically, and hypotonically induced corneal excitation. TRPV4-induced ATP release was attenuated by HC-06 and BAPTA-AM, demonstrating an obligatory link to $[Ca^{2+}]_i$ homeostasis and channel activation. Although previous studies linked epithelial ATP release to connexin and pannexin pores, vesicular exocytosis, P2X7 receptors, volume-regulated anion channels, and/or PI3K pathways,^{24,25,52,91–93} the sensitivity to probenecid accords with the pannexin rather than connexin, hemichannel mechanism. The prominent expression of Pnx1 in the mouse CE (Fig. 9)^{5,94} suggests a venue for Ca^{2+} -dependent release of ATP in the presence of calcium overloads from excessive stimulation of TRPV4, as well as potential release of neurotrophic factors and inflammatory mediators that are known to sensitize corneal nociceptors, and could regulate function of other tissues in the anterior eye (trabecular meshwork, ciliary body, stromal fibroblasts, corneal endothelium). TRPV4-evoked purinergic excitation drives the excitability of vagal and urothelial nociceptors.^{25,95} The ubiquity of TRPV4-dependent purinergic signaling across epithelia (including lung, kidney, ciliary body, gut, lens, bladder, and skin epithelia)^{24,51,92,96,97} further suggests that this mechanism might constitute a universal feature of epithelial sensory transduction.

CONCLUSIONS

We report that calcium homeostasis in native CECs is highly sensitive to extrinsic stressors, with TRPV4 and calcium mediating the effects of swelling and body temperature but not strain. The polymodal nonselective cation channel appears well placed to integrate physiological (osmotic gradients, fluid shear from eye blinks, temperature) and extrinsic (contact lens insertion, poking, chemical injury) inputs, a process that also involves epithelial release of ATP, a universal “danger” signal. It remains to be seen to what extent TRPV4 overactivation contributes to pathologies, such as corneal pain, edema, opacity, and epithelial inflammation. Because clinicians cannot always reliably distinguish between epithelial versus afferent nerve contributions to corneal pain, targeting epithelial sensory transduction might be useful to alleviate edema and/or hyperalgesic priming in dry eye disease, diabetes, glaucoma, and keratoconus as shown recently in brain and lung disease models, in which TRPV4 antagonists suppress edema, inflammation, and cell injury,^{81,86,98,99} and in the mouse cornea, in which TRPV4 ablation reduces inflammatory fibrosis.⁶⁹ Translational strategies will need to consider the possibility that impairing TRPV4-dependent release of neurotrophic peptides from CECs might affect afferent sensitivity, wound healing and repair,¹⁵ and that TRPV4-dependent release of modulatory factors impacts signaling mechanisms within the anterior eye.

Acknowledgments

The authors thank Wolfgang Liedtke (Duke University) for TRPV4^{-/-} mice, Maureen McCall (University of Louisville) for TRPV1^{tdT}, and Hongzhen Hu (Washington University School of Medicine) for TRPV4^{EGFP} mice.

Supported by the National Institutes of Health (R01EY022076, R01EY027920, P30EY014800), Willard L. Eccles Foundation, University of Utah Technology Acceleration Grant, the Neuroscience Initiative at the University of Utah (DK), Slovenian Research Agency (LL, MH); American Slovenian Education Foundation (LL, LG), Ad Futura Foundation (LL), and an Unrestricted Grant from Research to Prevent Blindness to the Department of Ophthalmology at the University of Utah. The authors alone are responsible for the content and writing of the article.

Disclosure: **L. Lapajne**, None; **M. Lakk**, None; **O. Yarishkin**, None; **L. Gubeljak**, None; **M. Hawlina**, None; **D. Križaj**, None

References

- Rozsa AJ, Beuerman RW. Density and organization of free nerve endings in the corneal epithelium of the rabbit. *Pain*. 1982;14:105–120.
- González-González O, Bech F, Gallar J, Merayo-Llodes J, Belmonte C. Functional properties of sensory nerve terminals of the mouse cornea. *Invest Ophthalmol Vis Sci*. 2017;58:404–415.
- Al Aqaba MA, Dhillon VK, Mohammed I, Said DG, Dua HS. Corneal nerves in health and disease. *Prog Retin Eye Res*. 2019;73:100762.
- Tomlinson A, Khanal S, Ramaesh K, Diaper C, McFadyen A. Tear film osmolarity: determination of a referent for dry eye diagnosis. *Invest Ophthalmol Vis Sci*. 2006;47:4309–4315.
- Minns MS, Teicher G, Rich CB, Trinkaus-Randall V. Purinoreceptor P2X7 regulation of Ca^{2+} mobilization and cytoskeletal rearrangement is required for corneal reepithelialization after injury. *Am J Pathol*. 2016;186:285–296.
- Masterton S, Ahearne M. Mechanobiology of the corneal epithelium. *Exp Eye Res*. 2018;177:122–129.
- Onochie OE, Zollinger A, Rich CB, Smith M, Trinkaus-Randall V. Epithelial cells exert differential traction stress in response to substrate stiffness. *Exp Eye Res*. 2019;181:25–37.
- Candia OA, Alvarez LJ. Fluid transport phenomena in ocular epithelia. *Prog Retin Eye Res*. 2008;27:197–212.
- Venkatachalam K, Montell C. TRP channels. *Annu Rev Biochem*. 2007;76:387–417.
- Sumioka T, Fujita N, Kitano A, Okada Y, Saika S. Impaired angiogenic response in the cornea of mice lacking tenascin C. *Invest Ophthalmol Vis Sci*. 2011;52:2462–2467.
- Yang Y, Yang H, Wang Z, Mergler S, Wolosin JM, Reinach PS. Functional TRPV1 expression in human corneal fibroblasts. *Exp Eye Res*. 2013;107:121–129.
- Mergler S, Garreis F, Sahlmuller M, Reinach PS, Paulsen F, Pleyer U. Thermosensitive transient receptor potential channels in human corneal epithelial cells. *J Cell Physiol*. 2011;226:1828–1842.
- Yamada T, Ueda T, Ugawa S, et al. Functional expression of transient receptor potential vanilloid 3 (TRPV3) in corneal epithelial cells: involvement in thermosensation and wound healing. *Exp Eye Res*. 2010;90:121–129.
- Pan Z, Yang H, Mergler S, et al. Dependence of regulatory volume decrease on transient receptor potential vanilloid 4 (TRPV4) expression in human corneal epithelial cells. *Cell Calcium*. 2008;44:374–385.

15. Okada Y, Sumioka T, Ichikawa K, et al. Sensory nerve supports epithelial stem cell function in healing of corneal epithelium in mice: the role of trigeminal nerve transient receptor potential vanilloid 4. *Lab Invest.* 2019;99:210–230.
16. Reinach PS, Mergler S, Okada Y, Saika S. Ocular transient receptor potential channel function in health and disease. *BMC Ophthalmol.* 2015;15(suppl 1):153.
17. Gevaert T, Vriens J, Segal A, et al. Deletion of the transient receptor potential cation channel TRPV4 impairs murine bladder voiding. *J Clin Invest.* 2007;117:3453–3462.
18. Sokabe T, Fukumi-Tominaga T, Yonemura S, Mizuno A, Tominaga M. The TRPV4 channel contributes to intercellular junction formation in keratinocytes. *J Biol Chem.* 2010;285:18749–18758.
19. Ueda T, Hoshikawa M, Shibata Y, Kumamoto N, Ugawa S. Basal cells express functional TRPV4 channels in the mouse nasal epithelium. *Biochem Biophys Res.* 2015;4:169–174.
20. Jo AO, Lakk M, Frye AM, et al. Differential volume regulation and calcium signaling in two ciliary body cell types is subserved by TRPV4 channels. *Proc Natl Acad Sci USA.* 2016;113:3885–3890.
21. Arredondo Zamarripa D, Noguez Imm R, Bautista Cortes AM, et al. Dual contribution of TRPV4 antagonism in the regulatory effect of vasoconstrictors on blood-retinal barrier permeability: diabetic milieu makes a difference. *Sci Rep.* 2017;7:13094.
22. Mihara H, Uchida K, Koizumi S, Moriyama Y. Involvement of VNUT-exocytosis in transient receptor potential vanilloid 4-dependent ATP release from gastrointestinal epithelium. *PLoS One.* 2018;13:e0206276.
23. Preston D, Simpson S, Halm D, et al. Activation of TRPV4 stimulates transepithelial ion flux in a porcine choroid plexus cell line. *Am J Physiol Cell Physiol.* 2018;315:C357–C366.
24. Mochizuki T, Sokabe T, Araki I, et al. The TRPV4 cation channel mediates stretch-evoked Ca²⁺ influx and ATP release in primary urothelial cell cultures. *J Biol Chem.* 2009;284:21257–21264.
25. Bonvini SJ, Birrell MA, Smith JA, Belvisi MG. Targeting TRP channels for chronic cough: from bench to bedside. *Naunyn-Schmiedeberg's Arch Pharmacol.* 2015;388:401–420.
26. Loukin S, Zhou X, Su Z, Saimi Y, Kung C. Wild-type and brachyolmia-causing mutant TRPV4 channels respond directly to stretch force. *J Biol Chem.* 2010;285:27176–27181.
27. Lechner SG, Markworth S, Poole K, et al. The molecular and cellular identity of peripheral osmoreceptors. *Neuron.* 2011;69:332–344.
28. Ryskamp DA, Jo AO, Frye AM, et al. Swelling and eicosanoid metabolites differentially gate TRPV4 channels in retinal neurons and glia. *J Neurosci.* 2014;34:15689–15700.
29. Toft-Bertelsen TL, Yarishkin O, Redmon S, Phuong TTT, Križaj D, MacAulay N. Volume sensing in the transient receptor potential vanilloid 4 ion channel is cell type-specific and mediated by an N-terminus volume-sensing domain. *J Biol Chem.* 2019;294:18421–18434.
30. Liedtke W, Friedman JM. Abnormal osmotic regulation in trpv4^{-/-} mice. *Proc Natl Acad Sci USA.* 2003;100:13698–13703.
31. Jo AO, Noel JM, Lakk M, et al. Mouse retinal ganglion cell signalling is dynamically modulated through parallel anterograde activation of cannabinoid and vanilloid pathways. *J Physiol.* 2017;595:6499–6516.
32. Gu QD, Moss CR, Kettelhut KL, Gilbert CA, Hu H. Activation of TRPV4 regulates respiration through indirect activation of bronchopulmonary sensory neurons. *Front Physiol.* 2016;7:65.
33. Phuong TTT, Redmon SN, Yarishkin O, Winter JM, Li DY, Križaj D. Calcium influx through TRPV4 channels modulates the adherens contacts between retinal microvascular endothelial cells. *J Physiol.* 2017;595:6869–6885.
34. Lakk M, Young D, Baumann JM, Jo AO, Hu H, Križaj D. Polymodal TRPV1 and TRPV4 sensors colocalize but do not functionally interact in a subpopulation of mouse retinal ganglion cells. *Front Cell Neurosci.* 2018;12:353.
35. Yarishkin O, Phuong TTT, Križaj D. Trabecular meshwork TREK-1 channels function as polymodal integrators of pressure and pH. *Invest Ophthalmol Vis Sci.* 2019;60:2294–2303.
36. Jo AO, Ryskamp DA, Phuong TTT, et al. TRPV4 and AQP4 channels synergistically regulate cell volume and calcium homeostasis in retinal muller glia. *J Neurosci.* 2015;35:13525–13537.
37. Lakk M, Yarishkin O, Baumann JM, Iuso A, Križaj D. Cholesterol regulates polymodal sensory transduction in Muller glia. *Glia.* 2017;65:2038–2050.
38. Ryskamp DA, Witkovsky P, Barabas P, et al. The polymodal ion channel transient receptor potential vanilloid 4 modulates calcium flux, spiking rate, and apoptosis of mouse retinal ganglion cells. *J Neurosci.* 2011;31:7089–7101.
39. Molnar T, Barabas P, Birnbaumer L, Punzo C, Kefalov V, Križaj D. Store-operated channels regulate intracellular calcium in mammalian rods. *J Physiol.* 2012;590:3465–3481.
40. Ryskamp DA, Frye AM, Phuong TTT, et al. TRPV4 regulates calcium homeostasis, cytoskeletal remodeling, conventional outflow and intraocular pressure in the mammalian eye. *Sci Rep.* 2016;6:30583.
41. Bandell M, Macpherson LJ, Patapoutian A. From chills to chilis: mechanisms for thermosensation and chemesthesis via thermoTRPs. *Curr Opin Neurobiol.* 2007;17:490–497.
42. Nakazawa Y, Donaldson PJ, Petrova RS. Verification and spatial mapping of TRPV1 and TRPV4 expression in the embryonic and adult mouse lens. *Exp Eye Res.* 2019;186:107707.
43. Mishra SK, Hoon MA. Ablation of TrpV1 neurons reveals their selective role in thermal pain sensation. *Mol Cell Neurosci.* 2010;43:157–163.
44. Alamri A, Bron R, Brock JA, Ivanusic JJ. Transient receptor potential cation channel subfamily V member 1 expressing corneal sensory neurons can be subdivided into at least three subpopulations. *Front Neuroanat.* 2015;9:71.
45. Liedtke W, Choe Y, Marti-Renom MA, et al. Vanilloid receptor-related osmotically activated channel (VR-OAC), a candidate vertebrate osmoreceptor. *Cell.* 2000;103:525–535.
46. Becker D, Bereiter-Hahn J, Jendrach M. Functional interaction of the cation channel transient receptor potential vanilloid 4 (TRPV4) and actin in volume regulation. *Eur J Cell Biol.* 2009;88:141–152.
47. Sharif Naeini R, Witty M-F, Seguela P, Bourque CW. An N-terminal variant of Trpv1 channel is required for osmosensory transduction. *Nat Neurosci.* 2006;9:93–98.
48. Zaelzer C, Hua P, Prager-Khoutorsky M, et al. DeltaN-TRPV1: a molecular co-detector of body temperature and osmotic stress. *Cell Rep.* 2015;13:23–30.
49. Scott JA. The computation of temperature rises in the human eye induced by infrared radiation. *Phys Med Biol.* 1988;33:243–257.
50. Guzman-Aranguiz A, Perez de Lara MJ, Pintor J. Hyperosmotic stress induces ATP release and changes in P2X7 receptor levels in human corneal and conjunctival epithelial cells. *Purinergic Signal.* 2017;13:249–258.
51. Mihara H, Suzuki N, Boudaka AA, et al. Transient receptor potential vanilloid 4-dependent calcium influx and ATP release in mouse and rat gastric epithelia. *World J Gastroenterol.* 2016;22:5512–5519.

52. Seminario-Vidal L, Okada SF, Sesma JI, et al. Rho signaling regulates Pannexin 1-mediated ATP release from airway epithelia. *J Biol Chem*. 2011;286:26277–26286.
53. Mihara H, Boudaka A, Sugiyama T, Moriyama Y, Tomi-naga M. Transient receptor potential vanilloid 4 (TRPV4)-dependent calcium influx and ATP release in mouse oesophageal keratinocytes. *J Physiol*. 2011;589:3471–3482.
54. Rahman M, Sun R, Mukherjee S, Nilius B, Janssen LJ. TRPV4 stimulation releases ATP via Pannexin channels in human pulmonary fibroblasts. *Am J Respir Cell Mol Biol*. 2018;59:87–95.
55. Bang S, Kim KY, Yoo S, Lee S-H, Hwang SW. Transient receptor potential V2 expressed in sensory neurons is activated by probenecid. *Neurosci Lett*. 2007;425:120–125.
56. Silverman W, Locovei S, Dahl G. Probenecid, a gout remedy, inhibits Pannexin 1 channels. *Am J Physiol Cell Physiol*. 2008;295:C761–C767.
57. Bond SR, Naus CC. The Pannexins: past and present. *Front Physiol*. 2014;5:58.
58. Sawatani T, Kaneko YK, Doutsu I, Ogawa A, Ishikawa T. TRPV2 channels mediate insulin secretion induced by cell swelling in mouse pancreatic beta-cells. *Am J Physiol Cell Physiol*. 2019;316:C434–C443.
59. Beckel JM, Argall AJ, Lim JC, et al. Mechanosensitive release of adenosine 5'-triphosphate through Pannexin channels and mechanosensitive upregulation of Pannexin channels in optic nerve head astrocytes: a mechanism for purinergic involvement in chronic strain. *Glia*. 2014;62:1486–1501.
60. Akazawa Y, Yuki T, Yoshida H, Sugiyama Y, Inoue S. Activation of TRPV4 strengthens the tight-junction barrier in human epidermal keratinocytes. *Skin Pharmacol Physiol*. 2013;26:15–21.
61. Martinez-Rendon J, Sanchez-Guzman E, Rueda A, et al. TRPV4 regulates tight junctions and affects differentiation in a cell culture model of the corneal epithelium. *J Cell Physiol*. 2017;232:1794–1807.
62. White JPM, Cibelli M, Urban L, Nilius B, McGeown JG, Nagy I. TRPV4: molecular conductor of a diverse orchestra. *Physiol Rev*. 2016;96:911–973.
63. Toft-Bertelsen TL, Križaj D, MacAulay N. When size matters: transient receptor potential vanilloid 4 channel as a volume-sensor rather than an osmo-sensor. *J Physiol*. 2017;595:3287–3302.
64. D'hoedt D, Owsianik G, Prenen J, et al. Stimulus-specific modulation of the cation channel TRPV4 by PACSIN 3. *J Biol Chem*. 2008;283:6272–6280.
65. Wegierski T, Lewandrowski U, Muller B, Sickmann A, Walz G. Tyrosine phosphorylation modulates the activity of TRPV4 in response to defined stimuli. *J Biol Chem*. 2009;284:2923–2933.
66. Galizia L, Pizzoni A, Fernandez J, Rivarola V, Capurro C, Ford P. Functional interaction between AQP2 and TRPV4 in renal cells. *J Cell Biochem*. 2012;113:580–589.
67. Sullivan MN, Francis M, Pitts NL, Taylor MS, Earley S. Optical recording reveals novel properties of GSK1016790A-induced vanilloid transient receptor potential channel TRPV4 activity in primary human endothelial cells. *Mol Pharmacol*. 2012;82:464–472.
68. Baratchi S, Keov P, Darby WG, et al. The TRPV4 agonist GSK1016790A regulates the membrane expression of TRPV4 channels. *Front Pharmacol*. 2019;10:6.
69. Okada Y, Shirai K, Miyajima M, et al. Loss of TRPV4 function suppresses inflammatory fibrosis induced by alkali-burning mouse corneas. *PLoS One*. 2016;11:e0167200.
70. Turker E, Garreis F, Khajavi N, et al. Vascular endothelial growth factor (VEGF) induced downstream responses to transient receptor potential vanilloid 1 (TRPV1) and 3-iodothyronamine (3-T1AM) in human corneal keratocytes. *Front Endocrinol (Lausanne)*. 2018;9:670.
71. Ryskamp DA, Redmon S, Jo AO, Križaj D. TRPV1 and endocannabinoids: emerging molecular signals that modulate mammalian vision. *Cells*. 2014;3:914–938.
72. Moran MM, Szallasi A. Targeting nociceptive transient receptor potential channels to treat chronic pain: current state of the field. *Br J Pharmacol*. 2018;175:2185–2203.
73. O'Leary C, McGahon MK, Ashraf S, et al. Involvement of TRPV1 and TRPV4 channels in retinal angiogenesis. *Invest Ophthalmol Vis Sci*. 2019;60:3297–3309.
74. Watanabe L, Fontes MRM, Soares AM, Giglio JR, Arni RK. Initiating structural studies of Lys49-PLA2 homologues complexed with an anionic detergent, a fatty acid and a natural lipid. *Protein Pept Lett*. 2003;10:525–530.
75. Marrelli SP, O'Neil RG, Brown RC, Bryan RMJ. PLA2 and TRPV4 channels regulate endothelial calcium in cerebral arteries. *Am J Physiol Heart Circ Physiol*. 2007;292:H1390–H1397.
76. Redmon SN, Shibasaki K, Križaj D. Transient receptor potential cation channel subfamily V member 4 (TRPV4). In: Choi S, ed. *Encyclopedia of Signaling Molecules*. Cham: Springer International Publishing; 2018:5665–5675.
77. Vriens J, Watanabe H, Janssens A, Droogmans G, Voets T, Nilius B. Cell swelling, heat, and chemical agonists use distinct pathways for the activation of the cation channel TRPV4. *Proc Natl Acad Sci USA*. 2004;101:396–401.
78. Martin E, Oliver KM, Pearce EI, Tomlinson A, Simmons P, Hagan S. Effect of tear supplements on signs, symptoms and inflammatory markers in dry eye. *Cytokine*. 2018;105:37–44.
79. Thiagarajah JR, Verkman AS. Aquaporin deletion in mice reduces corneal water permeability and delays restoration of transparency after swelling. *J Biol Chem*. 2002;277:19139–19144.
80. Iuso A, Križaj D. TRPV4-AQP4 interactions “turbocharge” astroglial sensitivity to small osmotic gradients. *Channels (Austin)*. 2016;10:172–174.
81. Hoshi Y, Okabe K, Shibasaki K, et al. Ischemic brain injury leads to brain edema via hyperthermia-induced TRPV4 activation. *J Neurosci*. 2018;38:5700–5709.
82. Hoffmann EK, Lambert IH, Pedersen SF. Physiology of cell volume regulation in vertebrates. *Physiol Rev*. 2009;89:193–277.
83. Murthy SE, Dubin AE, Whitwam T, et al. OSCA/TMEM63 are an evolutionarily conserved family of mechanically activated ion channels. *Elife*. 2018;7:e41844.
84. Thodeti CK, Matthews B, Ravi A, et al. TRPV4 channels mediate cyclic strain-induced endothelial cell reorientation through integrin-to-integrin signaling. *Circ Res*. 2009;104:1123–1130.
85. Servin-Vences MR, Moroni M, Lewin GR, Poole K. Direct measurement of TRPV4 and PIEZO1 activity reveals multiple mechanotransduction pathways in chondrocytes. *Elife*. 2017;6:e21074.
86. Pairet N, Mang S, Fois G, et al. TRPV4 inhibition attenuates stretch-induced inflammatory cellular responses and lung barrier dysfunction during mechanical ventilation. *PLoS One*. 2018;13:e0196055.
87. Matsumoto H, Sugio S, Seghers F, et al. Retinal detachment-induced muller glial cell swelling activates TRPV4 ion channels and triggers photoreceptor death at body temperature. *J Neurosci*. 2018;38:8745–8758.
88. Berna-Erro A, Izquierdo-Serra M, Sepúlveda R V, et al. Structural determinants of 5',6'-epoxyicosatrienoic acid binding to and activation of TRPV4 channel. *Sci Rep*. 2017;7:1–11.
89. Vriens J, Owsianik G, Janssens A, Voets T, Nilius B. Determinants of 4 alpha-phorbol sensitivity in transmembrane

- domains 3 and 4 of the cation channel TRPV4. *J Biol Chem*. 2007;282:12796–12803.
90. Goretzki B, Glogowski NA, Diehl E, et al. Structural basis of TRPV4 N terminus interaction with syndapin/PACSIN1-3 and PIP2. *Structure*. 2018;26:1583–1593.e5.
91. Praetorius HA, Leipziger J. ATP release from non-excitabile cells. *Purinergic Signal*. 2009;5:433–446.
92. Mamenko M, Zaika O, Jin M, O'Neil RG, Pochynyuk O. Purinergic activation of Ca²⁺-permeable TRPV4 channels is essential for mechano-sensitivity in the aldosterone-sensitive distal nephron. *PLoS One*. 2011;6:e22824.
93. Suadicani SO, Iglesias R, Wang J, Dahl G, Spray DC, Scemes E. ATP signaling is deficient in cultured Pannexin1-null mouse astrocytes. *Glia*. 2012;60:1106–1116.
94. Kurtenbach S, Kurtenbach S, Zoidl G. Emerging functions of Pannexin 1 in the eye. *Front Cell Neurosci*. 2014;8:263.
95. Aizawa N, Igawa Y, Andersson KE, Iijima K, Nishizawa O, Wyndaele JJ. Effects of intravesical instillation of ATP on rat bladder primary afferent activity and its relationship with capsaicin-sensitivity. *Neurourol Urodyn*. 2011;30:163–168.
96. Andrade YN, Fernandes J, Vazquez E, et al. TRPV4 channel is involved in the coupling of fluid viscosity changes to epithelial ciliary activity. *J Cell Biol*. 2005;168:869–874.
97. Delamere NA, Mandal A, Shahidullah M. The significance of TRPV4 channels and hemichannels in the lens and ciliary epithelium. *J Ocul Pharmacol Ther*. 2016;32:504–508.
98. Balakrishna S, Song W, Achanta S, et al. TRPV4 inhibition counteracts edema and inflammation and improves pulmonary function and oxygen saturation in chemically induced acute lung injury. *Am J Physiol Lung Cell Mol Physiol*. 2014;307:L158–L172.
99. Dalsgaard T, Sonkusare SK, Teuscher C, Poynter ME, Nelson MT. Pharmacological inhibitors of TRPV4 channels reduce cytokine production, restore endothelial function and increase survival in septic mice. *Sci Rep*. 2016;6:1–13.